Inorg. Chem. **2008**, *47*, 4570−4578

Interplay of Supramolecular Organization, Metallophilic Interactions, Phase Changes, and Luminescence in Four Polymorphs of $Ir^{I}(CO)_2(OC(CH_3)CHC(CH_3)N(p\text{-tol}))$

Emily M. Gussenhoven, Marilyn M. Olmstead, James C. Fettinger, and Alan L. Balch*

Department of Chemistry, University of California, Davis, California 95616

Received November 14, 2007

Four polymorphs of $Ir^{I}(CO)_2(OC(CH_3)CHC(CH_3)N(p\text{-tol}))$ have been characterized by single crystal X-ray crystallography. While all contain the same molecular unit with no significant structural variations within the molecules, all show different degrees of metallophilic interactions between the planar molecules. Three of these (the amber, the pale yellow, and the orange forms) are stable at room temperature, while the fourth, the L. T. orange form, is only obtained by cooling the orange polymorph. At 77 K, the amber, pale yellow, and L. T. orange polymorphs show intense luminescence. The variations in the luminescence among the polymorphs are considered in the context of the structural differences between them and the nature of the metallophilic interactions between the iridium centers. These results demonstrate how subtle variations in molecular organization can affect the physical properties of planar d^8 transition metal compounds, which are an important class of lumiphores.

Introduction

Polymorphs are isomers at the individual crystal level in which the same molecule or salt crystallizes in different fashions, which frequently, but not necessarily, result in differences in the space group and the cell dimensions.[1,2] In general, these polymorphs differ in such factors as the packing of the molecules and their relative orientation within the crystal, the conformations of the molecules, and the degree of ordering for highly symmetric molecules.[3,4] In such cases, the physical properties of each polymorph reflect the individual molecular character. However, when there are significant electronic interactions between the components that change in different polymorphs, there can be important changes in their properties.[5] For example, 4,4′,5,5′-tetramethyl-delta-2,2′-bi-1,3-diselenole-7,7,8,8-tetracyano-paraquinodimethane (TMTSF•TCNQ) forms two polymorphs.[6,7] The red form is a semiconductor that involves a mixed stack of donor and acceptor molecules, while the black polymorph is a conductor that crystallizes with segregated stacks of donors and acceptors. These observations proved the importance of segregated stacks in producing electrical conductivity in organic donor–acceptor cocrystals.

When two-coordinate d^{10} and four-coordinate d^8 complexes crystallize, self-association can result in the formation of significant metal−metal bonding between these complexes. These metallophilic interactions result from the overlap of the filled d_{z^2} orbitals and the empty p_z orbitals that lie along the direction of the metal−metal contact. These metallophilic interactions generally have chromophoric properties and can significantly alter the spectroscopic properties of the crystals.[8–10] Thus, this class of polymorphs has the ability to act as sensors that respond to environmental effects (temperature,[11] mechanical stress,[12] or the presence of organic vapors[13]) after crystal growth or during crystallization.[14]

* To whom correspondence should be addressed. E-mail: albalch@ucdavis.edu. Fax: 530-752-2820.

(1) Bernstein, J. *Polymorphism in Molecular Crystals*; Clarendon Press: Oxford, U.K., 2002.
(2) Dunitz, J. D.; Bernstein, J. *Acc. Chem. Res.* **1995**, *28*, 193–200.
(3) Braga, D.; Grepioni, F. *Chem. Soc. Rev.* **2000**, *29*, 229–238.
(4) Olmstead, M. M.; Jiang, F.; Balch, A. L. *Chem. Commun.* **2000**, *483*, 484.
(5) Bernstein, J. *J. Phys. D: Appl. Phys.* **1993**, *26*, 666–876.
(6) Kistenmacher, T. J.; Emge, T. J.; Bloch, A. N.; Cowan, D. O. *Acta Crystallogr., Sect. B: Struct. Sci.* **1982**, *B38*, 1193–1199.
(7) Bechgaard, K.; Kistenmacher, T. J.; Bloch, A. N.; Cowan, D. O. *Acta Crystallogr., Sect. B: Struct. Sci.* **1977**, *B33*, 417–422.
(8) Forward, J. M.; Fackler, J. P., Jr.; Assefa, Z. In *Optoelectronic Properties of Inorganic Compounds*; Roundhill, D. M., Fackler, J. P., Jr., Eds.; Plenum Press: New York, 1999; pp 195.
(9) Yam, V. W.-W. *Acc. Chem. Res.* **2002**, *35*, 555–563.
(10) Yam, V. W.-W.; Lo, K. K. W. *Chem. Soc. Rev.* **1999**, *28*, 323–334.
(11) Gussenhoven, E. M.; Fettinger, J. C.; Pham, D. M.; Malwitz, M. M.; Balch, A. L. *J. Am. Chem. Soc.* **2005**, *127*, 10838–10839.
(12) Lee, Y. A.; Eisenberg, R. *J. Am. Chem. Soc.* **2003**, *125*, 7778–7779.

10.1021/ic702243z CCC: $40.75
Published on Web 05/01/2008

Scheme 1

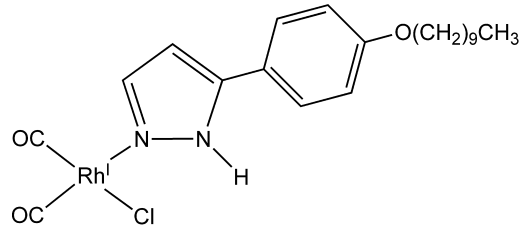

1, $Rh^{I}(CO)_2Cl(Hpz^{R})$

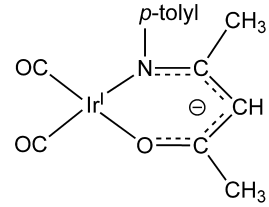

2, $Ir^{I}(CO)_2(OC(CH_3)CHC(CH_3)N(p\text{-tol}))$

There are only a few crystallographically characterized examples of polymorphs of planar, d^8 complexes that involve variations in the metallophilic interactions. The best known example, $Pt^{II}(2,2'\text{-bipyridine})Cl_2$, forms yellow and red polymorphs.[15,16] In the yellow form, the molecules are widely separated, and the platinum ions are isolated from each another.[17] In the red form, however, the molecules are arranged to form extended linear chains of platinum ions with a distance of 3.45 Å between adjacent platinum ions.[18] A different situation exists with $Rh^{I}(CO)_2Cl(Hpz^{R})$, **1** (see Scheme 1), where again yellow and red polymorphs form.[19] The yellow polymorph consists of dimers in which the planar molecules pack about a center of symmetry with a Rh···Rh separation of 3.3631 Å. In contrast, the red polymorph consists of a nearly linear (Rh···Rh···Rh angle, 178.86(5)°) chain of rhodium ions with Rh···Rh separations of 3.5296(5) Å.

Bonati and Ugo reported that $Ir^{I}(CO)_2(OC(CH_3)CHC(CH_3)N(p\text{-tol}))$ (**2**, see Scheme 1) and $Rh^{I}(CO)_2(OC(CH_3)CHC(CH_3)xN(p\text{-tol}))$ also formed both yellow and red crystals,[20] although they did not obtain crystallographic data on these. They suggested that the two forms might result from differing metal···metal interactions or various sorts of oligomerization to form out-of-plane M−O or M−N bonds. Here, we report crystallographic and spectroscopic studies that show that $Ir^{I}(CO)_2(OC(CH_3)CHC(CH_3)N(p\text{-tol}))$ forms four distinct polymorphs that have varying degrees of metallophilic interactions between the iridium centers and that exhibit strong luminescence at 77 K.

Results

Polymorph Crystallization. Samples of $Ir^{I}(CO)_2(OC(CH_3)CHC(CH_3)N(p\text{-tol}))$ were prepared following the procedure of Bonati and Ugo and purified by vacuum sublimation.[20] Vacuum sublimation of $Ir(CO)_2(OC(CH_3)CHC(CH_3)N(p\text{-tol}))$ produces yellow crystals that generally are tipped with smaller orange crystals. The sublimed material was not found to be suitable for X-ray diffraction. Recrystallization of the sublimed $Ir^{I}(CO)_2(OC(CH_3)CHC(CH_3)N(p\text{-tol}))$ from a pentane solution produced amber prisms, pale yellow plates, orange needles, and orange blocks concomitantly. Figure 1 shows photographs of these crystals. The orange needles grew more rapidly (over a 10 min period) while the amber prisms formed over a period of an hour. Large blocks of the orange crystals were also grown over 3 months from a dilute hexane solution at –15 °C (258 K). The pale yellow plates were most readily obtained through evaporation of a dilute pentane solution. The Experimental Section reports the most favorable conditions for obtaining each polymorph.

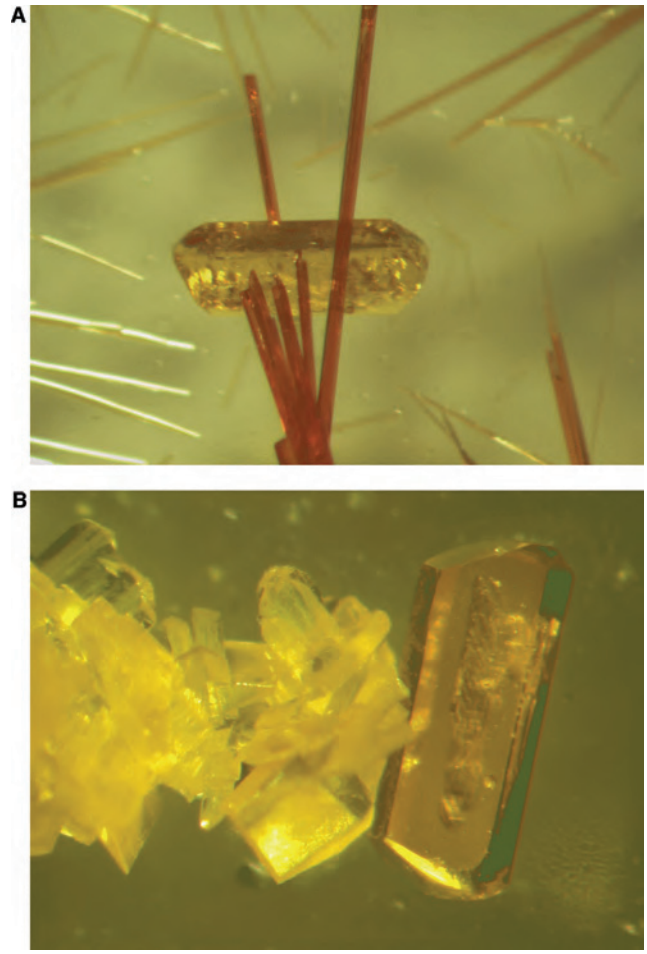

Figure 1. Photographs of crystals of the polymorphs of $Ir^{I}(CO)_2(OC(CH_3)CHC(CH_3)N(p\text{-tol}))$: (A) shows needles of the orange polymorph and an amber prism; (B) shows plates of the pale yellow polymorph and an amber prism.

(13) Lefebvre, J.; Batchelor, R. J.; Leznoff, D. B. *J. Am. Chem. Soc.* **2004**, *126*, 16117–16125.
(14) Braga, D.; Grepioni, F. *Angew. Chem., Int. Ed.* **2004**, *43*, 4002–4011.
(15) (a) Morgan, G. T.; Burstall, F. H. *J. Chem. Soc.* **1934**, 965. (b) Achar, S.; Catalano, V. J. *Polyhedron* **1997**, *16*, 1555.
(16) Grzesiak, A. L.; Matzger, A. J. *Inorg. Chem.* **2007**, *46*, 453.
(17) Herber, R. H.; Croft, M.; Coyer, M. J.; Bilash, B.; Sahiner, A. *Inorg. Chem.* **1994**, *33*, 2422.
(18) Osborn, R. S.; Rogers, D. *J. Chem. Soc., Dalton Trans.* **1974**, 1002.
(19) Torralba, M. C.; Cano, M.; Campo, J. A.; Heras, J. V.; Pinilla, E.; Torres, M. R. *J. Organomet. Chem.* **2001**, *91*, 633.
(20) Bonati, F.; Ugo, R. *J. Organomet. Chem.* **1967**, *7*, 167.

Table 1. Crystal Data and Data Collection Parameters for Polymorphs of $Ir^{I}(CO)_2(OC(CH_3)CHC(CH_3)N(p\text{-tol}))$

	amber	amber	pale yellow	pale yellow	orange	L. T. orange	L. T. orange
T (K)	296(2)	90(2)	296(2)	90(2)	298(2)	90(2)	20(2)
formula	$C_{14}H_{14}IrNO_3$	$C_{14}H_{14}IrNO_3$	$C_{14}H_{14}IrNO_3$	$C_{14}H_{14}IrNO_3$	$C_{14}H_{14}IrNO_3$	$C_{14}H_{14}IrNO_3$	$C_{14}H_{14}IrNO_3$
fw	436.46	436.46	436.46	436.46	436.46	436.46	436.46
color and habit	amber prism	amber prism	pale yellow plate	pale yellow plate	orange needle	orange needle	orange block
cryst syst	monoclinic	monoclinic	triclinic	triclinic	orthorhombic	monoclinic	monoclinic
space group	$P2_1/n$	$P2_1/n$	$P\bar{1}$	$P\bar{1}$	$Pnma$	$P2_1/n$	$P2_1/n$
a (Å)	9.2731(4)	9.2165(4)	9.5801(11)	9.4808(14)	13.614(7)	6.7754(6)	6.7210(7)
b (Å)	15.6736(7)	15.5357(7)	9.6759(11)	9.5679(14)	6.968(4)	13.3996(12)	13.3517(13)
c (Å)	10.0526(4)	9.8436(4)	15.6835(18)	15.416(2)	14.944(8)	14.9246(13)	14.8909(15)
α (deg)	90	90	87.985(2)	88.454(3)	90	90	90
β (deg)	93.4020(10)	93.8920(10)	83.837(2)	83.291(2)	90	90.0980(10)	90.053(5)
γ (deg)	90	90	88.304(2)	87.980(3)	90	90	90
V (Å^3)	1458.50(11)	1406.20(10)	1444.0(3)	1387.6(3)	1417.6(13)	1355.0(2)	1336.3(2)
radiation (λ, Å)	Mo Kα (0.71073)	Mo Kα (0.71073)	Mo Kα (0.71073)	Mo Kα (0.71073)	Mo Kα (0.71073)	Mo Kα (0.71073)	Mo Kα (0.71073)
Z	4	4	4	4	4	4	4
d_{calcd} (g•cm^{-3})	1.988	2.062	2.008	2.089	2.045	2.140	2.170
μ (mm^{-1})	9.156	9.497	9.248	9.625	9.421	9.856	9.994
no. of unique data	3361	4101	6668	6347	2223	3119	4352
no. of restraints	0	0	0	0	0	0	0
no. of params refined	176	175	350	350	111	176	176
R1[a]	0.019	0.014	0.047	0.0416	0.015	0.019	0.018
wR2[b]	0.052	0.035	0.131	0.109	0.040	0.049	0.040

[a] For data with $I \geq 2\sigma(I)$. $R1 = \sum||F_o| - |F_c||/\sum|F_o|$. [b] For all data. $wR2 = \sqrt{\sum[w(F_o^2 - F_c^2)^2]/\sum[w(F_o^2\sum F_c^2)^2]}$.

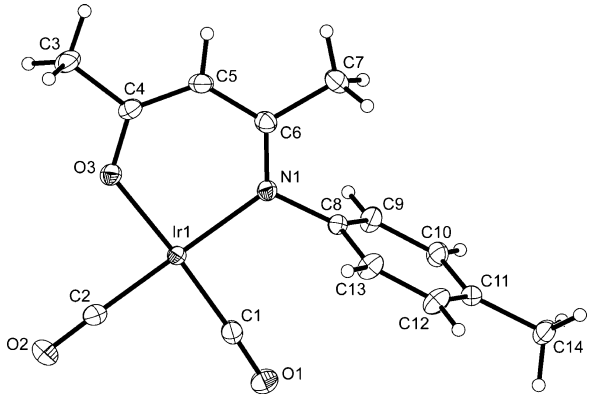

Figure 2. Drawing of the molecular structure of $Ir^{I}(CO)_2(OC(CH_3)CHC(CH_3)N(p\text{-tol}))$ in the amber polymorph at 90(2) K with 50% thermal contours. The structures of the molecules in the pale yellow and orange polymorphs are similar.

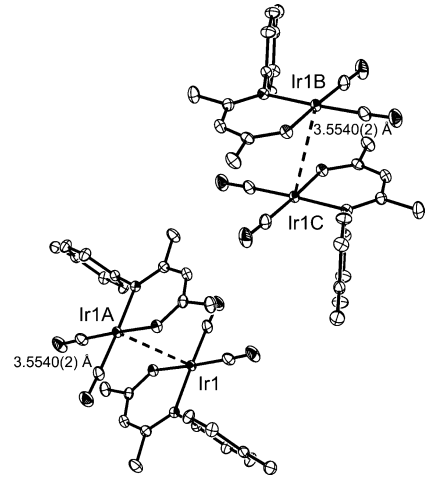

Figure 3. Drawing of two of the centrosymmetric dimers in the amber polymorph of $Ir^{I}(CO)_2(OC(CH_3)CHC(CH_3)N(p\text{-tol}))$ at 90(2) K with 50% thermal contours. The Ir···Ir distance is 3.5540(2) Å. The symmetry codes are as follows: 1A = $1 - x$, $1 - y$, $-z$; 1B = $0.5 - x$, $y + 0.5$, $-z - 0.5$; 1C = $x - 0.5$, $1.5 - y$, $z - 0.5$. Hydrogen atoms have been omitted for clarity.

Crystallographic Results for the Polymorphs of $Ir^{I}(CO)_2(OC(CH_3)CHC(CH_3)N(p\text{-tol}))$. The structures of the amber, pale yellow, and orange polymorphs that form from pentane solutions of $Ir^{I}(CO)_2(OC(CH_3)CHC(CH_3)N(p\text{-tol}))$ have been determined by X-ray crystallography both at room temperature (298(2) or 296(2) K) and at 90(2) K. At 90(2) K, the orange polymorph, which is found as either needles or blocks, has undergone a phase transition, yielding a fourth polymorph, the L. T. orange polymorph. Data collection of this form was also carried out at 20(2) K.

Amber Polymorph. The amber polymorph crystallizes in the monoclinic space group $P2_1/n$ with one molecule in the asymmetric unit. Crystal data are given in Table 1. For this polymorph, the structure is essentially the same at room temperature and at 90(2) K.

Figure 2 shows a drawing of the molecule in the amber polymorph at 90(2) K. Selected bond distances and angles are given in Table 2. The complex has the expected planar structure with *cis* carbonyl ligands and a chelating β-ketoiminato group surrounding the iridium ion. At 90(2) K, the plane of the phenyl substituent makes a dihedral angle of 93.8° with regard to the plane of the IrC_2NO group.

Figure 3 shows a drawing of the interactions between the molecules in the amber polymorph. The molecules form dimers that are packed about a center of symmetry. The interactions between the monomers will be characterized by the Ir···Ir distances, the interplanar separations, and the lateral shifts as defined in Scheme 2. These parameters are

Scheme 2. Interplanar Separation and Lateral Shift

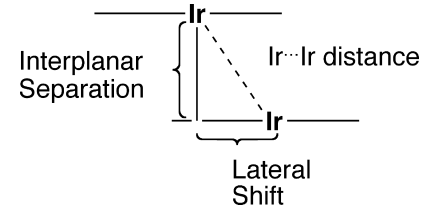

Table 2. Selected Bond Distances and Angles for $Ir^{I}(CO)_2(OC(CH_3)CHC(CH_3)N(p\text{-tol}))$

	amber	amber	pale yellow	pale yellow	orange	L. T. orange	L. T. orange
T (K)	296(2)	90(2)	296(2)	90(2)	298(2)	90(2)	20(2)
Distance (Å)							
Ir1−C1	1.829(4)	1.840(2)	1.839(13)	1.845(11)	1.831(3)	1.838(4)	1.842(3)
Ir1−C2	1.847(4)	1.858(2)	1.853(14)	1.858(10)	1.849(4)	1.855(4)	1.854(3)
Ir1−O3	2.022(2)	2.0236(15)	2.006(7)	2.022(6)	2.024(2)	2.033(2)	2.031(2)
Ir1−N1	2.053(3)	2.058(2)	2.054(9)	2.045(8)	2.064(3)	2.065(3)	2.063(2)
Ir1···Ir1#1	3.6609(3)	3.5540(2)	3.7362(9)	3.5934(8)	3.6055(18)	3.4126(5)	3.3402(4)
Ir2···Ir2#2			4.1264(10)	4.0397(8)		3.6237(5)	3.6396(4)
interplanar separation	3.5696(16)	3.4634(9)	3.607(5)	3.473(4)	3.484(2)	3.347(2)	3.2959(14)
			3.857(6)	3.771(5)		3.419(2)	3.406(2)
lateral shift	0.8125	0.7971	0.975	0.923	0.9281	0.667	0.5422
			1.467	1.449		1.201	1.2829
Ir2−C15			1.845(14)	1.855(11)			
Ir2−C16			1.862(14)	1.861(10)			
Ir2−O6			2.032(7)	2.028(6)			
Ir2−N2			2.052(9)	2.063(8)			
Ir2−Ir2#1			4.1264(10)	4.0397(8)			
angle (deg)							
M(1A)···M(1)···M(1B)	none	none	none	none	150.16(2)	148.682(9)	148.667(7)

given in Table 2. At 90(2) K, the monomers interact through an Ir···Ir contact of 3.5540(2) Å, while the separation between the planes of a pair of adjacent molecules is 3.4634(9) Å. The next closest iridium ion is 7.5824(3) Å from Ir1 at 90(2) K. At 296(2) K, the Ir···Ir distance lengthens appreciably to 3.6609(3) Å, while the interplanar separation also increases to 3.5696(16) Å.

Pale Yellow Polymorph. The pale yellow polymorph crystallizes in the triclinic space group $P\bar{1}$ with two molecules in the asymmetric unit. The angles between the plane of the phenyl ring and the plane of the IrC_2NO unit in the two molecules are 91.6° (Ir1) and 86.9° (Ir2). No significant changes in molecular structure were observed between the structures obtained at 296(2) and 90(2) K. Bond distances and angles are reported in Table 2. Each of the two molecules closely resembles the molecule in the amber polymorph shown in Figure 2, but the packing interactions between the molecules differ. Figure 4 shows the interactions between the four closest molecules in the solid. As with the amber polymorph, pairs of molecules in the pale yellow polymorph make face-to-face contacts that result from packing about centers of symmetry. In one pair, the Ir1···Ir1A separation is 3.5934(8) Å, which is slightly longer than the corresponding distance in the amber polymorph. However, in the second pair, the Ir2···Ir2A separation is considerably larger, 4.0397(8) Å. On warming to 296(2) K, these two distances increase significantly to 3.7362(9) Å for Ir1···Ir1A and 4.1264(10) Å for Ir2···Ir2A. The lateral shifts for the two pairs differ; at 296(2) K, they are 0.975 and 1.467 Å for the pairs containing Ir1 and Ir2, respectively. Consequently, the degree of overlap between the pairs of molecules differs.

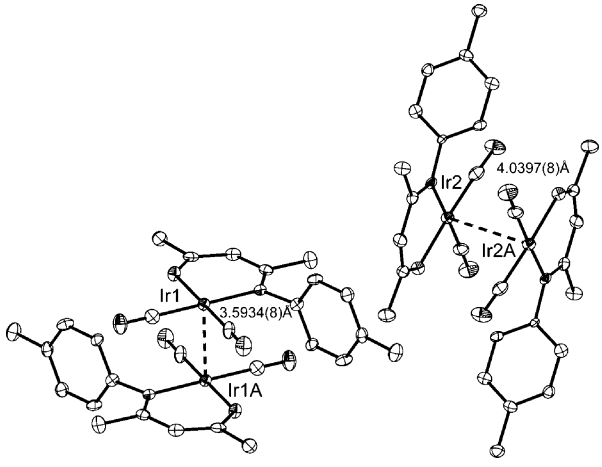

Figure 4. Drawing of two dimers in the pale yellow polymorph of $Ir^{I}(CO)_2(OC(CH_3)CHC(CH_3)N(p\text{-tol}))$ at 90(2) K with 50% thermal contours. The Ir···Ir distances are 3.5934(8) and 4.0397(8) Å. The symmetry codes are as follows: 1A = $-x, -y, -z$; 2A = $1-x, 1-y, 1-z$.

Orange Polymorphs. At room temperature, the orange polymorph crystallizes in the orthorhombic space group *Pnma*. Both the needle and the block morphologies yield the same structure. These crystals undergo a phase change upon cooling, and the low-temperature form will be designated as the L. T. (low temperature) orange polymorph. At room temperature, the orange polymorph contains one-half of a molecule in the asymmetric unit. The other half is generated by reflection. A crystallographic mirror plane contains all of the non-hydrogen atoms except for the ortho and meta carbon atoms of the *p*-tolyl group. The structure of the molecule in the orange polymorph is similar to that in the amber polymorph, as may be appreciated by examining the bond distances and angles presented for both polymorphs in Table 2. Here crystallographic symmetry dictates that the *p*-tolyl substituent is oriented perpendicular to the plane of the iridium complex.

In the orange polymorph at 298(2) K, the monomers form extended chains, as seen in Figure 5A. There are centers of symmetry between each pair of iridium atoms in the chain. Thus, each pair of adjacent molecules has a local structure similar to that of the discrete dimers seen in the amber polymorph. These kinked chains of iridium ions have an Ir1A···Ir1···Ir1B angle of 150.2° and propagate along the *b* axis of the crystal. The Ir···Ir separation is 3.6055(18) Å, which is slightly longer than that seen for the dimers in the amber polymorph. The interplanar separation between the monomers in these chains is 3.484(2) Å. Thus, as a result of this kinking, the Ir···Ir separation is longer than the interplanar separation between the monomers.

Cooling the orange crystals results in a gradual phase change, which is reflected by slight changes in the crystal-

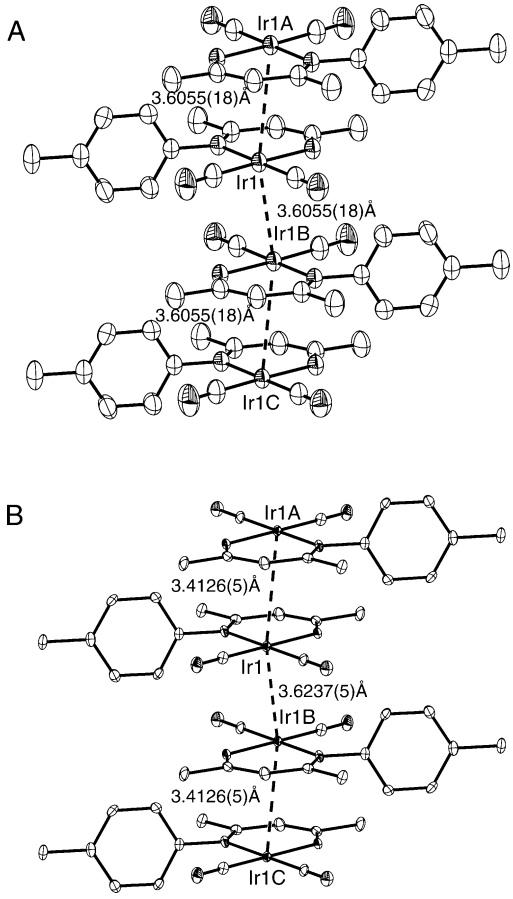

Figure 5. Drawing of the columnar structure: (A) in the orange polymorph of $Ir^{I}(CO)_2(OC(CH_3)CHC(CH_3)N(p\text{-tol}))$; (B) in the L. T. orange polymorph of $Ir^{I}(CO)_2(OC(CH_3)CHC(CH_3)N(p\text{-tol}))$. Thermal ellipsoids were drawn at 40% for both the high- and low-temperature forms. Symmetry codes for part A: 1A = $1-x, -y, 1-z$; 1B = $1-x, 0.5+y, 1-z$; 1C = $x, 1+y, z$. Symmetry codes for part B: 1A = $-x, -y, -z$; 1B = $1-x, -y, -z$; 1C = $1+x, y, z$. The Ir···Ir distances are 3.6055(18) Å in the orange polymorph and 3.4126(5) and 3.6237(5) Å in the L. T. orange polymorph.

lographic parameters but not in the color of the crystal. At 90(2) K, the crystal is monoclinic, space group $P2_1/n$. In the L. T. orange polymorph, the asymmetric unit consists of an entire molecule with no crystallographically imposed symmetry. Nevertheless, the molecule is essentially planar, and its dimensions are essentially identical to those found in the amber, the pale yellow, and the orange polymorphs, as seen from the data in Table 2.

Although the molecular structures are similar in the two orange polymorphs, there are significant differences in the molecular packing, which affect the chemical interactions between the monomers. Figure 5B shows how the molecules are arranged in the L. T. orange polymorph to give a columnar structure. Within the columns of the L. T. orange polymorph, the Ir···Ir separations alternate so that pairs of iridium ions are separated by 3.4126(5) and 3.6237(5) Å, respectively, at 90(2) K. Similarly, the interplanar separations within a column alternate between 3.347(2) and 3.419(2) Å, with the shorter distance corresponding to the molecules with the shorter Ir···Ir separation of 3.4126(5) Å. Upon cooling the crystal to 20(2) K, the difference between the two Ir···Ir separations (3.3402(4) and 3.6396(4) Å) increases, although

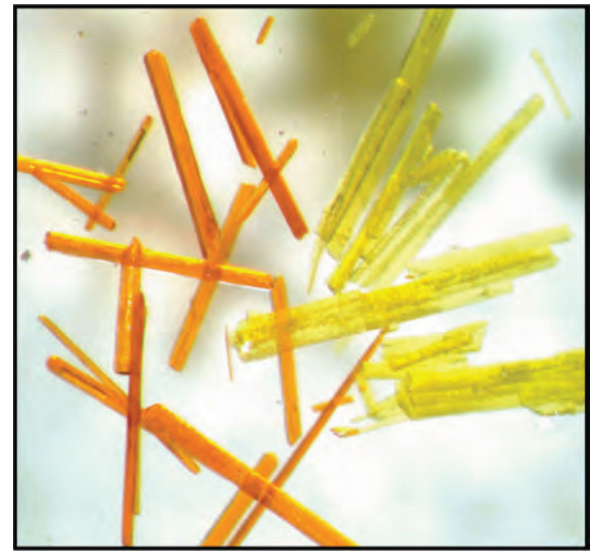

Figure 6. Photograph of the needles of the orange polymorph of $Ir^{I}(CO)_2(OC(CH_3)CHC(CH_3)N(p\text{-tol}))$ before (on the left) and after (on the right) heating to 115 °C (388 K).

the crystal maintains the monoclinic $P2_1/n$ space group found at 90(2) K. Whereas the orange polymorph has a uniform lateral shift of 0.923 Å along the chain, at 90(2) K, the L. T. orange polymorph has two different lateral shifts, one (1.201 Å) that is longer than in the orange polymorph and one (0.667 Å) that is shorter.

Interconversions of Polymorphs of $Ir^{I}(CO)_2(OC(CH_3)CHC(CH_3)N(p\text{-tol}))$. Warming of the L. T. orange crystals results in their conversion back to the orange phase with identical X-ray diffraction at 298(2) K. At room temperature, however, the amber, the pale yellow, and the orange polymorphs of $Ir^{I}(CO)_2(OC(CH_3)CHC(CH_3)N(p\text{-tol}))$ appear to be indefinitely stable. Recrystallization of a homogeneous sample of these polymorphs from a pentane solution produces a mixture of all three polymorphs. Heating a sample of the amber polymorph produces no changes until the sample melts at 154–155 °C (427–428 K). Similarly, heating a sample of the pale yellow polymorph results in its simple melting at 155–156 °C (428–429 K). However, heating a sample of the orange polymorph results in its conversion into the amber form at 107–110 °C (379–383 K). Further heating of this sample results in its melting at 155–158 °C (428–431 K), which is in the temperature range where the pale yellow and amber polymorphs melt.

Figure 6 shows crystals of the orange polymorph before and after heating at 115 °C (388 K). Heating converts the orange needles into yellow needles with striations that run perpendicular to the needle axis. The yellow needles produced by heating have been examined crystallographically and were found to have cell dimensions similar to those of the amber polymorph, although the crystal quality of the thermally treated needles is much poorer than that of solution grown amber polymorph.

Figure 7 shows the difference in the molecular packing between the orange and the amber polymorphs. The orange polymorph contains the complexes stacked into bent chains, while the amber polymorph is constructed of discrete dimers.

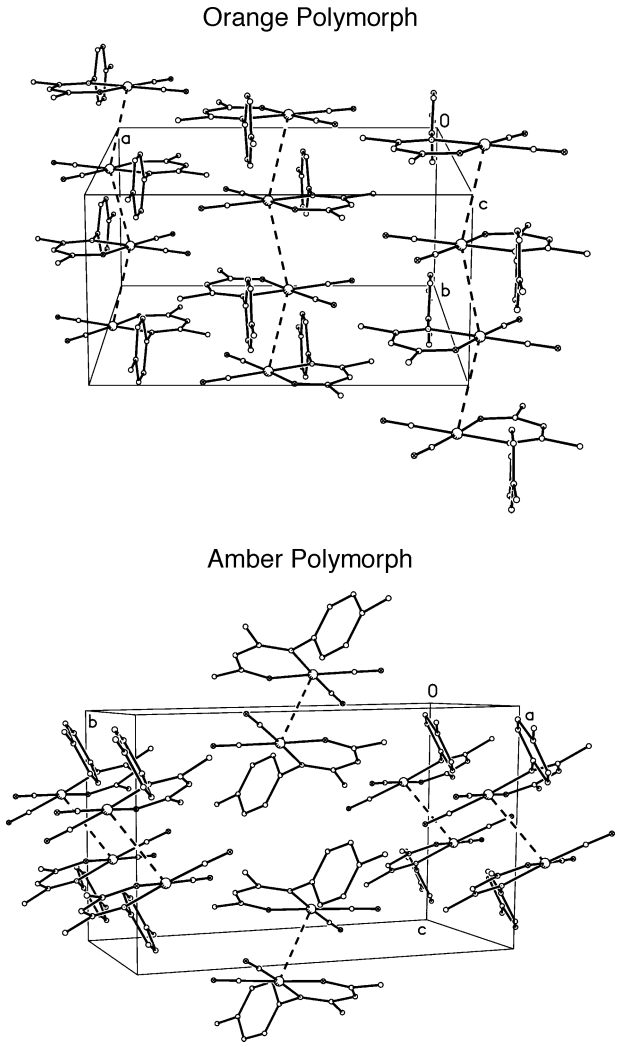

Figure 7. Comparison of the molecular packing in the orange polymorph and the amber polymorph of Ir^{I}(CO)$_2$(OC(CH$_3$)CHC(CH$_3$)N(*p*-tol)) at room temperature.

As Figure 7 reveals, adjacent dimer pairs in the amber polymorph are tipped with respect to one another so that there is no columnar organization as seen in the orange polymorph.

Considerable reorganization is needed to convert the orange polymorph into the amber one. The required molecular dislocations are clearly larger than the rather small readjustments needed to transform the orange polymorph into the L. T. orange polymorph, as can be appreciated by viewing Figure 5.

Spectroscopic Properties of the Polymorphs of Ir^{I}(CO)$_2$(OC(CH$_3$)CHC(CH$_3$)N(*p*-tol)). The UV/vis absorption spectra of solutions of the pale yellow, the amber, and the orange polymorph are shown in Figure 8. As this figure shows, all three forms dissolve in dichloromethane to form pale yellow solutions that have identical UV/vis spectra with a low energy maximum at 385 nm (ε = 675 M^{-1} cm^{-1}). However, the absorption spectra of these crystalline polymorphs differ from the solution spectra. The solid-state UV/vis spectrum of the amber polymorph at 298 K shows a prominent absorption at 329 nm and a low energy absorption maximum at 420 nm. Crystals of the pale yellow polymorph show similar features at 329 and 420 nm, while the orange

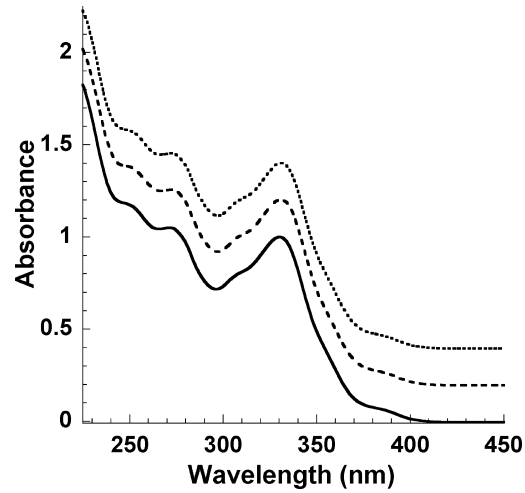

Figure 8. UV/vis absorption spectra of dichloromethane solutions of the amber (dotted line), the pale yellow (dashed line), and the orange (solid line) polymorphs of Ir^{I}(CO)$_2$(OC(CH$_3$)CHC(CH$_3$)N(*p*-tol)) at 298 K.

polymorph shows corresponding absorbances at 330 and 496 nm. These low energy features are not present in the absorption spectra taken in solution. Consequently, these low energy features of the crystals reflect the metallophilic interactions between the complexes that occur in the solid state and probably are a result of the weak Ir···Ir interactions between the individual molecules.

Dichloromethane solutions prepared from each of these polymorphs are not luminescent. Additionally, the crystalline solids are not luminescent at room temperature. However, crystals of the pale yellow, the amber, and the L. T. orange polymorphs are strongly luminescent at 77 K, as the data in Figure 9 show. At 77 K, the amber polymorph shows an emission maximum at 654 nm with a structured excitation spectrum centered at 431 nm and Stokes' shifts of 0.98 eV. Under the same conditions, the pale yellow polymorph exhibits emission at 635 nm with a structured excitation centered at 427 nm and a Stokes' shift of 0.95 eV. At 77 K the L. T. orange polymorph displays a red emission with λ_{max} of 770 nm. The excitation profile for this emission shows a maximum at 504 nm with a Stokes shift of 0.85 eV. The emission lifetimes for the three polymorphs at 77 K are similar in magnitude: amber, 10(1) μs; pale yellow, 11(1) μs; L. T. orange, 14(1) μs. Consideration of the lifetimes and the sizable Stokes shifts for the emissions suggests that the luminescence of each polymorph arises from phosphorescence.

The infrared spectra of the room temperature stable polymorphs also show some variations. The amber polymorph exhibits ν(CO) at 2054 (sh), 2045, 1969, and 1946 (sh) cm^{-1} and two bands at 1515 and 1504 cm^{-1} in the 1600–1500 cm^{-1} region. The pale yellow polymorph has ν(CO) at 2058 (sh), 2043, 1979 (sh), 1972, and 1949 (sh) cm^{-1} and bands at 1518 and 1504 cm^{-1} in the 1600–1500 cm^{-1} region. The orange polymorph displays ν(CO) at 2045 (sh), 2038, 2021 (sh), 1965, and 1934 (sh) cm^{-1} and four bands at 1564, 1556 (sh), 1515 (sh), and 1505 cm^{-1} in the 1600–1500 cm^{-1} region.

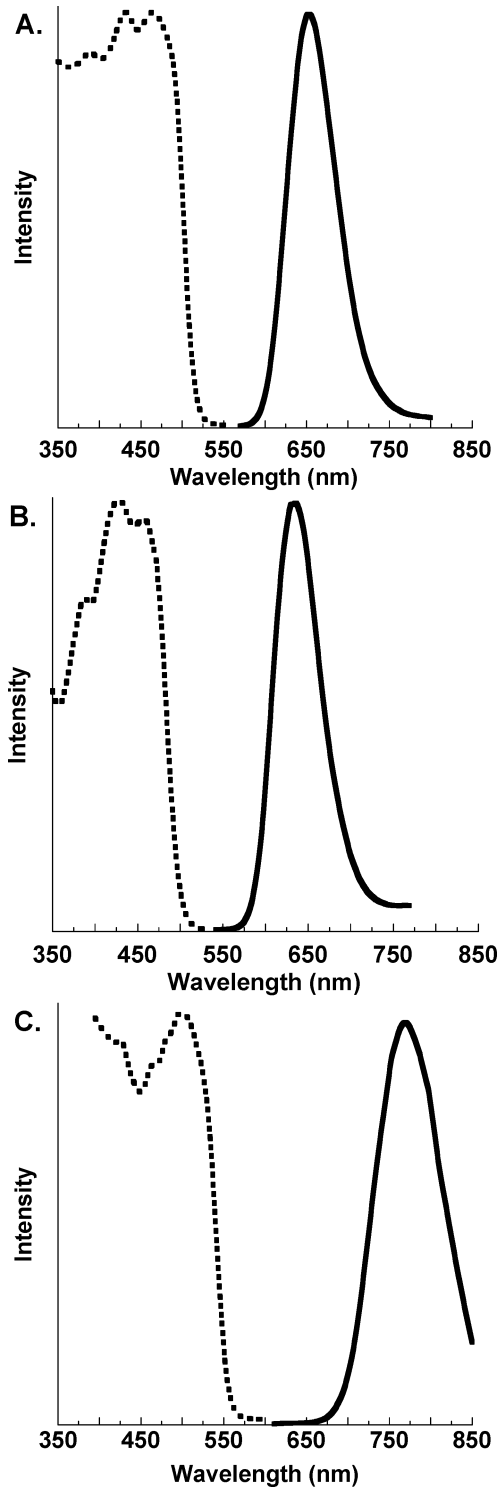

Figure 9. Corrected emission (solid lines) and corrected excitation (dotted lines) spectra of crystalline samples of polymorphs of $Ir^{I}(CO)_2(OC(CH_3)CHC(CH_3)N(p\text{-tol}))$ at 77 K: (A) amber polymorph (emission, $\lambda_{max} = 654$ nm; excitation, $\lambda_{max} = 390$, 431, and 465 nm); (B) pale yellow polymorph (emission, $\lambda_{max} = 635$ nm, excitation, $\lambda_{max} = 388$, 427, and 459 nm); (C) orange polymorph (emission, $\lambda_{max} = 770$ nm, excitation, $\lambda_{max} = 504$ nm).

Discussion

Four polymorphs of $Ir^{I}(CO)_2(OC(CH_3)CHC(CH_3)N(p\text{-tol}))$ have been identified; three (the amber, the pale yellow, and the orange) are stable at room temperature, while the fourth, the L. T. orange form, is only obtained by cooling the orange polymorph. Thus, this system is more complex than is the case with the other two planar, d^8 complexes, Pt^{II}(2,2′-bipyridine)Cl_2 or $Rh^{I}(CO)_2Cl(Hpz^{R})$, where only two polymorphs have been found for each complex. Moreover, with $Ir^{I}(CO)_2(OC(CH_3)CHC(CH_3)N(p\text{-tol}))$, we have been able to observe direct thermal conversions between some of the polymorphs. While the orange polymorph is reversibly converted into the L. T. orange polymorph upon cooling, heating the orange polymorph at 115 °C (388 K) results in its functionally irreversible conversion into the amber polymorph.

Comparison of our results with those of Bonati and Ugo[20] reveals that the infrared spectrum they report for their yellow polymorph shows fairly good agreement with the data we obtained for the amber and pale yellow forms. On the other hand, the infrared spectrum that Bonati and Ugo reported for their red polymorph (ν(CO) bands at 2062, 2046, 1991, and 1973 cm^{-1}) is significantly different from the data we report for the orange polymorph (ν(CO) 2045, 2038, 2021(sh), 1965, and 1934 cm^{-1}). Bonati and Ugo reported that their red polymorph converted to the yellow form by heating above 120 °C (393 K), while we found that the orange form transformed into the amber phase over the temperature range 107–110 °C (379–383 K). Moreover, Bonati and Ugo noticed that their red polymorph gradually converted into a yellow form upon standing for a few months at room temperature, but we have not seen any instability in our orange form at room temperature. Indeed, in this laboratory, a sample of the orange polymorph has been stored for a year without signs of transformation to another form. For their yellow polymorph, Bonati and Ugo reported a melting point of 155 °C (428 K), while we found that the amber polymorph melted over the range 154–155 °C (427–428 K), and the pale yellow phase melted over the range 154–155 °C (427–428 K). We conclude that the yellow form of Bonati and Ugo could be either the amber or the pale yellow forms we report here or a mixture of the two. Differentiation between these two polymorphs is difficult. Indeed, it was only in the latter stages of our investigations that we discovered that there were distinct amber and pale yellow forms present. On the other hand, the differences between the data reported for the red polymorph of Bonati and Ugo and the data for our orange polymorph suggest that these may be different and that there may be a fifth polymorph lurking in the wings that we have not been able to reproduce. It is well-known that polymorphs have a tendency to disappear.[2]

The molecular structure of $Ir^{I}(CO)_2(OC(CH_3)CHC(CH_3)N(p\text{-tol}))$ in each polymorph is similar, as the data in Table 2 show. However, the packing and the interactions between molecules differ. The molecules are most widely spaced in the pale yellow polymorph, where the separations between the two pairs of molecules that show close approach are 3.7362(9) Å for Ir1···Ir1A and 4.1264(10) Å for Ir2···Ir2A at 296(2) K; these distances decrease to 3.5934(8) and 4.0397(8) Å, respectively, at 90(2) K.

The Ir···Ir separations in all forms of $Ir^{I}(CO)_2(OC(CH_3)CHC(CH_3)N(p\text{-tol}))$ are rather long but are shorter than 4.0

Å, which is twice the van der Waals radius for Ir, according to recent calculations.[21,22] Moreover, no other interactions (such as $\pi-\pi$ overlap or hydrogen bonding) are found that hold the dimers and chains together. For comparison, the Ir···Ir separation in $Ir^{I}(CO)_2(OC(CH_3)CHC(CH_3)O(CH_3))$, which has an extended linear chain structure, is much shorter, 3.20 Å.[23] Racemic $Ir^{I}(CO)_2$(6-trifluoroacetylcarvonato) forms dimers with a Ir···Ir distance of 3.290(1) Å.[24] The red salts $(Et_4N)[Ir^{I}(CO)_2(Tcbiim)]$, $(Et_2Me_2N)[Ir^{I}(CO)_2(Tcbiim)]$, and $(Et_2Me(CH_2)_4NEt_2MeN)$-$[Ir^{I}(CO)_2(Tcbiim)]$, where Tcbiim is the dianion 4,4′,5,5′-tetracyano-2,2′-biimidazolate, form extended stacks with Ir···Ir separations of 3.154, 3.206, and 3.159 Å, respectively, whereas the yellow salt (Et_3MeN)-$[Ir^{I}(CO)_2(Tcbiim)]$ appears to have no substantial metallophilic interactions with the closest contact between the iridium centers of 4.036 Å.[25] The shortest Ir···Ir distance in $Ir^{I}(CO)_2Cl$(pyrazine), which also forms extended stacks, is 3.579(3) Å.[26]

The calculated densities of the polymorphs at 90(2) K reveal that the L. T. orange phase is the densest and thus the most efficiently packed, while the amber form is the least dense. At room temperature a similar trend exists with the orange phase the densest, while the amber form is the least dense. In their study of the red and yellow polymorphs of $Pt(bpy)Cl_2$ and $Pt(phen)Cl_2$, Grzesiak and Matzger concluded that Pt···Pt interactions interfered with close packing and that the yellow polymorphs which had no significant Pt···Pt interactions were more densely packed.[16] In contrast with $Ir^{I}(CO)_2(OC(CH_3)CHC(CH_3)N(p\text{-tol}))$, it is the polymorph with the most extensive and shortest Ir···Ir interactions that produces the densest phases at both 90(2) K and room temperature. The pale yellow polymorph of $Ir^{I}(CO)_2(OC(CH_3)$-$CHC(CH_3)N(p\text{-tol}))$, which is the polymorph with the longest Ir···Ir separations, has an intermediate density.

The absorption and emission spectra of these complexes reveal that there are spectroscopically significant interactions between the individual molecules even at the rather long separations seen here. All of the room temperature stable polymorphs show absorption maxima that occur at lower energies than the absorption seen in solution. Thus, the lowest energy absorption features are ascribed to transitions from the filled, out-of-plane iridium d_{z^2} orbitals to the empty p_z orbitals. At 77 K, the amber, the pale yellow, and the L. T. orange polymorphs are all luminescent, as the data in Figure 9 show. The emission and excitation spectra of the amber and pale yellow polymorphs are similar. This similarity probably reflects the similarity in the structure of the two crystals. Both crystals contain a face-to-face pair of $Ir^{I}(CO)_2$-$(OC(CH_3)CHC(CH_3)N(p\text{-tol}))$ molecules with similar Ir···Ir separations: 3.5934(8) Å for the pale yellow form and 3.5540(2) Å for the amber polymorph. We believe that it is these pairs that are involved in producing the emission. In the pale yellow polymorph, the second pair of molecules with an Ir···Ir separation of 4.0397(8) Å is too widely separated to allow any significant overlap of the out-of-plane d_{z^2} and p_z orbitals, and consequently, this pair is unlikely to contribute to the emission behavior. Note that, despite the presence of two different pairs of molecules, only a single emission is seen for the pale yellow polymorph.

The emission from the L. T. orange polymorph occurs at a significantly lower energy than that seen for the pale yellow and the amber polymorphs, and the excitation maximum also occurs at a lower energy. These changes can be ascribed to the fact that the L. T. orange polymorph contains an extended chain of interacting iridium centers. As a result of the contribution from many such centers, the energy gap between the filled iridium d_{z^2} levels and the empty iridium p_z levels is lowered. Consequently, the excitation maximum for the L. T. orange polymorph occurs at a lower energy than the excitation maximum for the amber or yellow polymorph.

The phase change of the orange polymorph into the L. T. orange polymorph results in an interesting alternation of the interactions within an extended chain. At 296(2) K, all of the separations in a chain are the same. Upon cooling to 90(2) K, one Ir···Ir distance contracts as might be expected, but the other Ir···Ir separation expands slightly. Cooling to 20(2) K produces further contraction of one Ir···Ir separation, while the other Ir···Ir separation expands further. There are many examples of extended linear chain compounds with equivalent metal···metal separations along the chain,[27] and there are also numerous examples of extended chain complexes where the metal···metal separations alternate between long and short.[28] However, to our knowledge this is the first case where a reversible process converts a chain with equivalent metal···metal separations into one with alternating long and short metal···metal separations.

The phase change involving the orange polymorph and the L. T. orange polymorph does have some features in common with another phase change that alters metal···metal interactions. The trinuclear cation in $[\mu_3\text{-}S(AuCNC_7H_{13})_3]$-$(SbF_6)$ undergoes self-association in the solid state to produce a dimer with a pseudo-octahedral array of six gold atoms.[11] On cooling, a phase change occurs that lowers the symmetry of the gold cations and results in the creation of two different pairs of cations: one with contracted interionic Au···Au separations and the other with expanded interionic Au···Au

(21) Nag, S.; Banerjee, K.; Datta, D. *New J. Chem.* **2007**, *31*, 832.
(22) Batsanov, S. S. *Inorg. Mater.* **2001**, *37*, 871.
(23) Pitt, C. G.; Monteith, L. K.; Ballard, L. F.; Collman, J. P.; Morrow, J. C.; Roper, W. R.; Ulkü, D. *J. Am. Chem. Soc.* **1966**, *88*, 4286.
(24) Scheer, P.; Schurig, V.; Walz, L. *Acta Crystallogr., Sect. C: Cryst. Struct. Commun.* **1990**, *C46*, 1442.
(25) Rasmussen, P. G.; Kolowich, J. B.; Bayoñ, J. C. *J. Am. Chem. Soc.* **1988**, *110*, 7042.
(26) Dragonetti, C.; Pizzotti, M.; Roberto, D.; Galli, S. *Inorg. Chim. Acta* **2002**, *330*, 128.
(27) (a) For example: $Rh^{I}(CO)_2Cl$(*N*-methylimidazole); Rh···Rh, 3.4522(4) Å. Bonati, F.; Oro, L. A.; Pinillos, M. T.; Tejel, C.; Apreda, M. C.; Foces-Foces, C.; Cano, F. H. *J. Organomet. Chem.* **1989**, *369*, 253. (b) $Rh^{I}(CO)_2(OC(CF_3)CHC(Ph)O)$; Rh···Rh, 3.537 Å. Leipoldt, J. G.; Bok, L. D. C.; Basson, S. S.; van Vollenhoven, J. S.; Gerber, T. I. A. *Inorg. Chim. Acta* **1977**, *25*, L63. (c) $Rh^{I}(CO)_2Cl$(pyrazole); Rh···Rh, 3.4522(4) Å. Decker, M. J.; Fjeldsted, D. O. K.; Stobart, S. R.; Zaworotko, M. J. *J. Chem. Soc., Chem. Commun* **1983**, 1525.
(28) (a) For example: $Rh^{I}(CO)_2Cl$(pyridine); Rh···Rh, 3.479, 4.029 Å. Heaton, B. T.; Jacob, C.; Sampanthar, J. T. *J. Chem. Soc., Dalton Trans.* **1998**, 1403. (b) $Rh^{I}(CO)_2(OC(CH_3)CHC(CH_3)O)$; Rh···Rh, 3.253, 3.271 Å. Huq, F. A. C. *J. Cryst. Mol. Struct.* **1974**, *4*, 411. (c) $[Pt^{II}$(4′-(p-nicotinamide-*N*-methylphenyl)-2,2′:6′,2″-terpyridine)$Cl](PF_6)_2$; Pt···Pt, 3.301, 3.360 Å. Wadas, T. J.; Wang, Q.-M.; Kim, Y.; Flaschenreim, C.; Blanton, T. N.; Eisenberg, E. *J. Am. Chem. Soc.* **2004**, *126*, 16841.

separations. The phase change for this gold cluster affects its luminescence. At high temperature, a single emission is seen, whereas, at temperatures below the phase change, two emissions are observed, one from the contracted cluster and one from the expanded cluster. In contrast, the L. T. orange polymorph of $Ir^{I}(CO)_2(OC(CH_3)CHC(CH_3)N(p\text{-tol}))$ exhibits only a single emission, since the emission arises from a section of the extended chain rather than from discrete dimeric sites within the chain.

The study of polymorphs of inorganic and organometallic compounds has the potential to produce new solids and functional materials whose physical properties are altered because of the intermolecular organization.[3] The present work and the results reported in related papers[11,29,30] demonstrate that polymorph formation can have a significant influence on metal−metal bonding. These results demonstrate how the luminescence of solids can be altered by varying the intermolecular interactions through polymorph formation.

Experimental Section

Materials. $Ir^{I}(CO)_2(OC(CH_3)CHC(CH_3)N(p\text{-tol}))$ was prepared following the procedure of Bonati and Ugo[20] and purified by vacuum sublimation.

Crystallization of the Polymorphs of $Ir^{I}(CO)_2(OC(CH_3)CHC(CH_3)N(p\text{-tol}))$. The sublimed solids (111 mg, 20% yield) obtained from the preparation of $Ir^{I}(CO)_2(OC(CH_3)CHC(CH_3)N(p\text{-tol}))$ were dissolved in 20 mL of boiling pentane. The solution was filtered, concentrated to approximately 10 mL, and covered, and the solvent was allowed to evaporate slowly. Concomitant polymorphs were obtained as orange needles and amber prisms developed from the same solution, with crystallization initiated by the former polymorph. The orange needles grew rapidly over 10 min, while the amber prisms formed over approximately 1 h. It is possible to produce mainly crystals of the orange polymorph or only of the pale yellow polymorph by changing the concentration of the solution, altering the evaporation rate, or using seed crystals. However, a method has not yet been developed for obtaining quantities of the amber polymorph in its entirety. For example, concentrating the initial pentane solution to approximately 2 mL and allowing the solvent to evaporate in an uncovered beaker will produce a batch of approximately 98% orange needles and 2% amber prisms. Alternatively, large blocks of the orange crystals can also be grown over 3 months in a dilute hexane solution (ca. 20 mg in 35 mL) at 258 K. In order to produce predominately pale yellow plates (with ca. 2% formation of the amber polymorph), 20 mL of a pentane solution of the complex was allowed to slowly evaporate over 5–8 h in a covered beaker. When this dilute solution was seeded with some of the pale yellow plates, the pale yellow form was produced in nearly 100% yield. To generate a sample of mainly amber prisms (mixed with ca. 20% pale yellow plates), a dilute solution was seeded with three crystals of the amber polymorph collected from a previous batch. Physical properties were measured on homogeneous samples of the individual polymorphs that were separated by hand.

Physical Measurements. Infrared spectra were recorded as neat powders on a Mattson Genesis II FT-IR spectrometer fitted with a Specac ATR accessory. Electronic absorption spectra were recorded using a PharmaSpec UV-1700 UV–visible spectrophotometer. Spectra of solids were obtained from samples dispersed in Nujol mulls. Corrected emission and excitation spectra were taken on polycrystalline samples with a SPEX FluoroMax-3 spectrofluorometer manufactured by Jobin Yvon/HORIBA.

X-ray Crystallography and Data Collection. For the low-temperature experiments, at 20(2) or 90(2) K, the crystals were removed from the beakers in which they were grown and immediately coated with hydrocarbon oil on microscope slides. Suitable crystals were mounted on glass fibers with silicone grease and placed in a cold stream of either a Bruker SMART CCD or a Bruker SMART ApexII diffractometer. Dinitrogen (90(2) K) and helium (20(2) K) cooling were accomplished by use of CRYO Industries devices. For high-temperature experiments (296(2) or 298(2) K), the crystals were mounted with Super Glue onto glass fibers attached to metal pins; these assemblies were placed on the goniometer head of the diffractometer for data collection. The crystal structures were solved by direct methods, and all data were refined (based on F^2) using SHELXTL 5.1 software. A multiscan method utilizing equivalents was employed to correct for the absorption of heavy atoms.[31] Hydrogen atoms were located in a difference map, added geometrically, and refined with a riding model. Crystallographic data, selected bond lengths, and angles, together with metallophilic geometry, are collected in Tables 1 and 2.

For the pale yellow crystal structures at 296(2) and 90(2) K, a correction for rotational twinning was applied using TwinRotMat;[32] the twin parameters were refined to 0.0448(10) and 0.0671(10), respectively. The structure for the L. T. orange block at 20(2) K was refined as a pseudomerohedral twin, with a twin law of [−1 0 0 0 −1 0 0 0 1] and a twin parameter that refined to 0.3955(7). For the orange polymorph, at 298(2) K, the structure contains a molecule in which the methyl groups involving C3 and C7 are oriented each with one hydrogen in the mirror plane. For the L. T. orange polymorph, there are several indications that the correct space group is monoclinic $P2_1/n$, and not orthorhombic *Pnma*, as was found at 298(2) K for the orange polymorph. At 90(2) K, in the space group *Pnma*, there are approximately 2% of the strong reflections that are systematic absence violations; however, there were no violations for $P2_1/n$. In addition, at 90(2) K, refinement of several of the lighter atoms with anisotropic thermal parameters leads to nonpositive definite values in *Pnma* but not in $P2_1/n$. Furthermore, the wR2 value in *Pnma* is approximately double the wR2 value in $P2_1/n$. In the space group $P2_1/n$, a satisfactory refinement was obtained by application of the twin law [−1 0 0 0 −1 0 0 0 1] and the refinement of the twin parameter to a value of 0.2535(15).

Acknowledgment. We thank the Petroleum Research Fund (Grant No. 37056-AC) for support and the Tyco Foundation for a fellowship for E.M.G. The Bruker SMART 1000 diffractometer was funded in part by NSF Instrumentation Grant No. CHE-9808259.

Supporting Information Available: X-ray crystallographic files in cif format for the amber, pale yellow, orange, and L. T. orange polymorphs of $Ir^{I}(CO)_2(OC(CH_3)CHC(CH_3)N(p\text{-tol}))$. This material is available free of charge via the Internet at http://pubs.acs.org.

IC702243Z

(29) White-Morris, R. L.; Olmstead, M. M.; Balch, A. L. *J. Am. Chem. Soc.* **2003**, *125*, 1033.
(30) White-Morris, R. L.; Olmstead, M. M.; Attar, S.; Balch, A. L. *Inorg. Chem.* **2005**, *44*, 5021.
(31) Sheldrick, G. M. *SADABS 2007/2*; University of Göttingen: Göttingen, Germany, 2007.
(32) Spek, A. L. *PLATON 2007*; University of Utrecht: Utrecht, The Netherlands, 2007.